

EFFECT OF THE FUEL INJECTION PRESSURE ON THE COMBUSTION PROCESS IN A PFI BOOSTED SPARK-IGNITION ENGINE

S. S. Merola, P. Sementa, C. Tornatore, B. M. Vaglieco

Istituto Motori - CNR

Via G. Marconi, 8 - 80125 Napoli Italy, e-mail: s.merola@im.cnr.it

Abstract

In this paper, low-cost solutions were proposed to reduce the fuel consumption in a boosted port fuel injection spark ignition (PFI SI) engine, taking into account the engine performances and the pollutants emission. To this purpose, the optical characterization of the fuel injection and of the combustion process was carried out in a PFI SI engine. The experiments were performed on a partially transparent single-cylinder SI engine, equipped with a four-valve head and an external boost device. The intake manifold was optically accessible through three holes that allowed the introduction of an endoscope and of optical fibres.

The standard injection condition planned by the engine manufacturer was investigated, it consisted in the fuel injection at 3.5 bar when the intake valves were closed. Moreover, the fuel injection with open intake valves was tested; 3.5 and 6.5 bar fuel pressures were studied for open and closed valves conditions. Optical techniques based on 2D-digital imaging were used to follow the fuel injection spray in the intake manifold and the flame propagation in the combustion chamber. The results of in-cylinder optical investigations were correlated with the engine performances and with the exhaust emissions.

Keywords: PFI SI Engine; Boosting; Fuel Injection; Fuel deposition; Optical diagnostics

1. Introduction

In spite of the sharp oil prices and of the global pollution increase, actually the adoption of alternative engine technologies is not widespread. In fact, hybrids and electric vehicles are familiar for a meagre share of the worldwide market. While the US and Canada consumers are used to the hybrids cars, these are totally alien to the new market as Chinese and Indian one. Thus the introduction of the very low-emission vehicles should run parallel to the optimization of the internal combustion engines. For the gasoline engines, to respect the future stringent legislation, the overall emissions levels decrease should be coupled with a strong reduction in fuel consumption. In the last years, the request of high-performance cars together with the use of the catalyst light-off strategies and engine calibrations for the hydrocarbon and NO_x emissions reduction increased the fuel consumption of the gasoline spark ignition (SI) engines. To remedy it was necessary the downsizing and boosting of the SI engines. It allowed the increase in power and torque without the increase in cylinder capacity. The reduction in the engine capacity at the same power gave strong benefits in terms of fuel consumption due to the reduction in pumping-losses. Moreover the lower engine capacity limited the gases-to-wall heat transfer due to a reduced internal surface area and to a shorter flame travel distance. Finally, lower friction losses were obtained thanks to smaller moving parts. Thus, the optimization of the boosted SI engines is one of the starting points for the development of a more eco-sustainable internal combustion engine. In this work, low-cost solutions to improve the combustion efficiency of a boosted port fuel injection (PFI) SI engines were proposed. In particular, the increase in the fuel injection pressure was tested in the open valves and closed valves conditions.

The experiments were realised in a partially transparent single-cylinder PFI SI engine with an external boosting device. The engine was equipped with a four-valve real engine head and fuelled with commercial gasoline. The optical investigations performed in the intake manifold and in the cylinder were correlated with the engine performance and with the exhaust emissions.

2. Experimental apparatus

2.1. Transparent Engine

Fig. 1 reports the sketch of the apparatus for the experimental activities. It was used an optically accessible single cylinder PFI SI engine equipped with the cylinder head of the new generation SI turbocharged engine. The engine details are reported in Tab. 1.

A ten-hole injector was employed. It provided a spray pattern quite symmetric with respect to the wall dividing the intake ducts. Fig. 2 reports the drawing of the injector holes configuration.

The head had four valves and a centrally located spark plug. A quartz pressure transducer was flush-installed to measure the in-cylinder pressure.

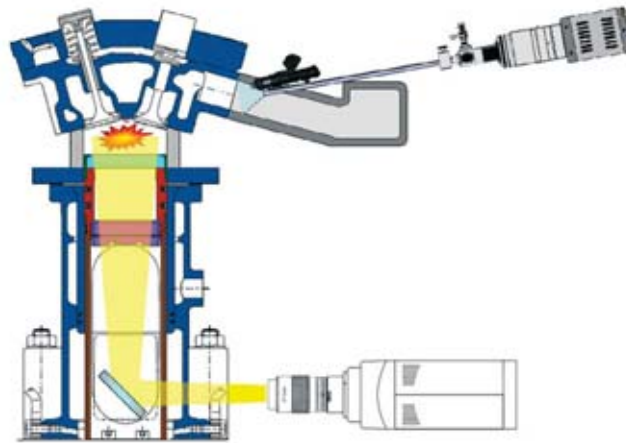


Fig. 1. Experimental apparatus for optical investigations in the intake manifold and in the combustion chamber



Fig. 2. Drawing of injector holes configuration

Tab. 1. Specifications of the single cylinder PFI SI engine

Displacement	399 cm ³
Bore	79.0 mm
Stroke	81.3 mm
Connecting road	143 mm
Compression ratio	10:1

The in-cylinder pressure, the rate of chemical energy release and the related parameters were evaluated on an individual cycle basis and/or averaged on 400 cycles [1].

The engine piston was flat and transparent through a 57 mm diameter quartz window. To reduce the window contamination by lubricating oil, an elongated piston arrangement was used together with unlubricated Teflon-bronze composite piston rings in the optical section.

An external device controlled the intake air pressure in a range of 1000-2000 mbar and the temperature in a range of 290-340 K.

2.2. Optical setup

The jet visualization was investigated in the intake manifold using an endoscope coupled with a 12-bit digital CCD colour camera. The fuel spray was illuminated by flash cold pulsed light source through an optical fibre. The CCD had a 640 x 480 pixel matrix with a pixel size of 9.9 x 9.9 μm^2 . This optical assessment allowed a spatial resolution of 90 $\mu\text{m}/\text{pixel}$. The CCD spectral range was 290-800 nm.

During the combustion process, the light passed through a UV-fused silica window located in the piston and it was reflected toward the optical detection assembly by a 45° inclined UV-visible mirror located in bottom of the engine. Then the light was focused by a 78 mm focal length, f/3.8 UV Nikon objective on an intensified cooled CCD (ICCD) camera. The ICCD had an array size of 512 x 512 pixels and 16-bit dynamic range. The ICCD spectral range was 180-700 nm.

For all the optical measurements, the synchronization between the cameras and the engine was made by the crank angle encoder signal through a unit delay. The exposure time of the cameras was fixed at 41.6 μs that corresponds to 0.5 crank angle degrees (CAD) at engine speed of 2000 rpm. The dwell time between two consecutive images was set at 41.6 μs .

3. Results and discussion

3.1. Engine Operating Conditions

All the tests presented in this paper were carried out at engine speed of 2000 rpm and wide open throttle (WOT). The absolute intake air pressure and the temperature were fixed at 1400 mbar and 323 K, respectively.

Tab. 2. Engine operating conditions

TEST	Inj. pressure [bar]	Duration of Inj. [CAD]	Start of Inj. vs TDC [CAD]
CV1_L	3.5	142	130
CV1_H	6.5	109	130
OV1_L	3.5	138	-300
OV1_H	6.5	104	-300

Several fuel injection strategies were considered. In particular, closed valves (CV1) and open valves (OV1) conditions were investigated for two injection pressures: 3.5 and 6.5 bar. For all the test cases, the duration of the injection was chosen to obtain stoichiometric equivalence ratio, as measured by a lambda sensor at the engine exhaust. The spark timing was fixed to operate always in the Maximum Brake Torque (MBT) condition [2]. More details about the engine operating conditions are reported in Tab. 2. Fig. 3 (a) shows the values of the Indicated Mean Effective Pressure (IMEP) evaluated for the selected operating conditions on 400 consecutive cycles. The error bars are referred to the related IMEP coefficient of variation. IMEP and COV resulted good and comparable with those measured for a real multi-cylinder engine[3]. Fig. 3 (b) reports the Brake Specific Fuel Consumption (BSFC) values.

As it can be noted, the improvement of the injection pressure determined a little reduction in performance and a decrease in consumption. In order to better understand the thermo-fluid dynamic phenomena that induced this effect, detailed optical investigations were performed.

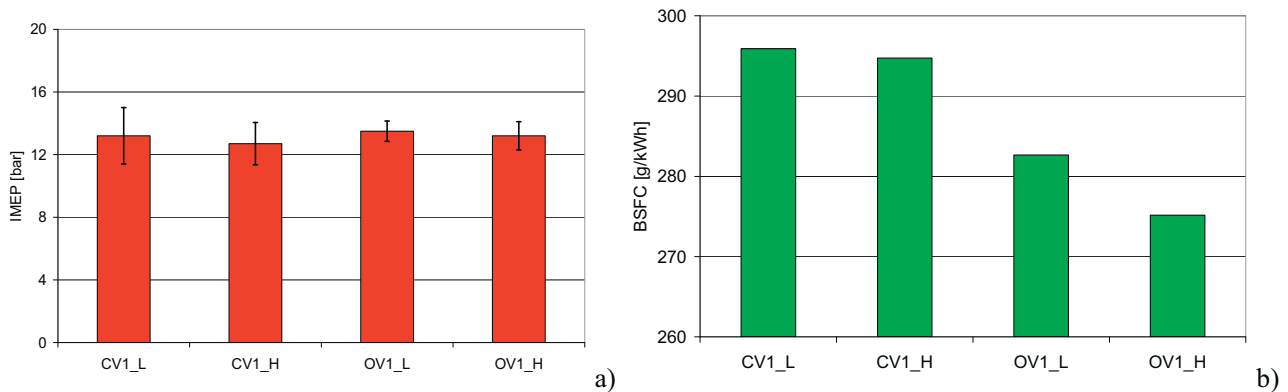


Fig. 3. (a) IMEP and (b) BSFC measured for the selected operating conditions

3.2. Injection Analysis

The injection characterisation in the intake manifold was carried out with two different endoscopes positioned at 90° and 180° with respect to the manifold axis.

Fig. 4-5 report the spray evolution in the intake manifold realized at 180° point of view for all the injection strategies investigated. The five jets on each side of the injector could not be resolved by imaging. It can be observed that only two fuel jets were distinguishable and the injection pressure affected the jet cone angle and penetration for all the cases. In particular, the cone angle increased at increasing injection pressure. This effect was due to the low air-motion and it was more evident in the closed valves condition. Moreover, as expected, the fuel jet penetration rose more rapidly and stabilized at a highest value in the highest pressure condition. Conversely, the digital imaging realized at 90° point of view with respect to manifold axis showed that the injection pressure had no effects on the jet penetration axis. In particular, at 3.5 bar, the two jet cores resulted well separated and the fuel droplets were always well resolved in the images until the end of the injection. This demonstrated that the droplets mean diameter was higher than the imaging spatial resolution. At 6.5 bar, from 4 ms after the SOI, the droplets resulted a sort of cloud in the intake manifold and their mean size could not be evaluated. This effect was induced by a better fuel atomization.

In the open valves conditions (Fig. 5), the jets cone angle was smaller than in the closed valves ones. From the images obtained at 180° point of view it was noted that the open valves conditions showed the jet closer to the intake manifold wall and its axis was inclined with respect to the injector axis. This effect was reduced by the increase in the injection pressure. Moreover, on the spray right side, a more penetrating jet was observed and its cone angle was greater than the left side one.

All these phenomena were affected by the intake-flow field evolution towards the combustion chamber during the engine cycle. It had direct effects on the spray morphology and it influenced the fuel mixing, the vaporization and the amount of fuel deposited on the intake manifold.

In the open valves case, at low pressure, the incipient closing of the intake ports, which occurred around 12 ms, determined an entrapment of small fuel droplets amount in the intake manifold. During the engine cycle, the droplets impinged on the walls and on the intake valves causing fuel film deposits. As shown in Fig. 4-5, the injection pressure had a similar effect on the droplets distributions in the closed and open valves conditions even if in the latter condition, the number of droplets appeared lower. These effects are well evident in Fig. 6, which reports the comparison between the binary digitisations of the fuel sprays detected in the closed valves condition at 8 ms from SOI for the selected injection pressures.

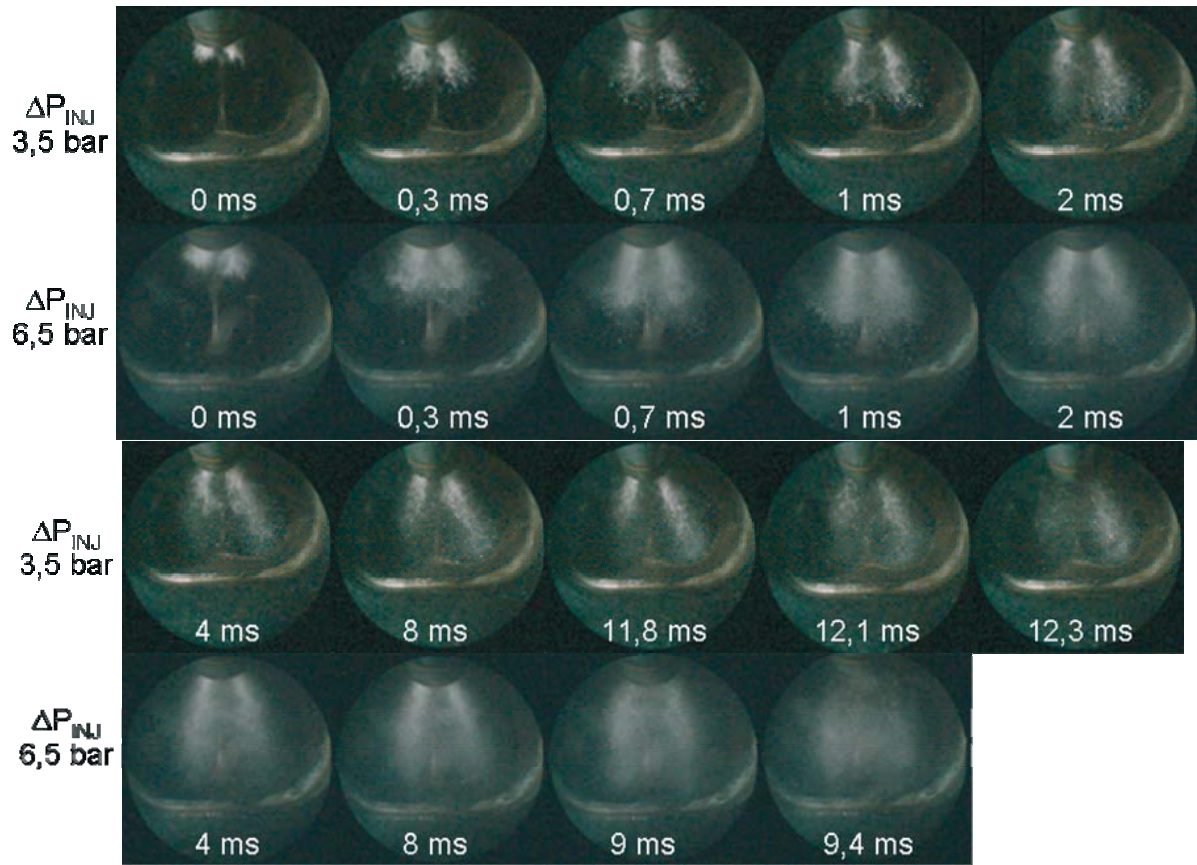


Fig. 4. Injection images detected in the intake manifold for the closed valves strategy at 180° point of view

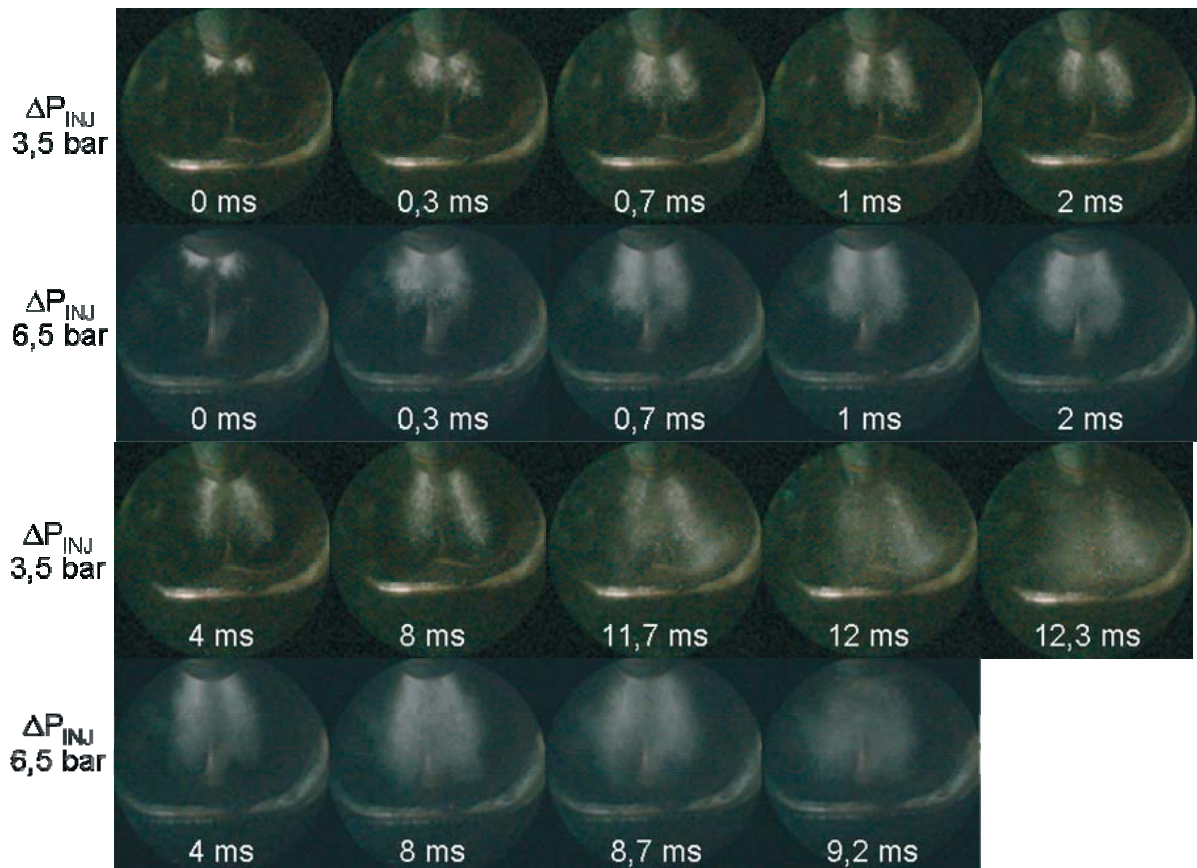


Fig. 5. Injection images detected in the intake manifold for the open valves strategy at 180° point of view

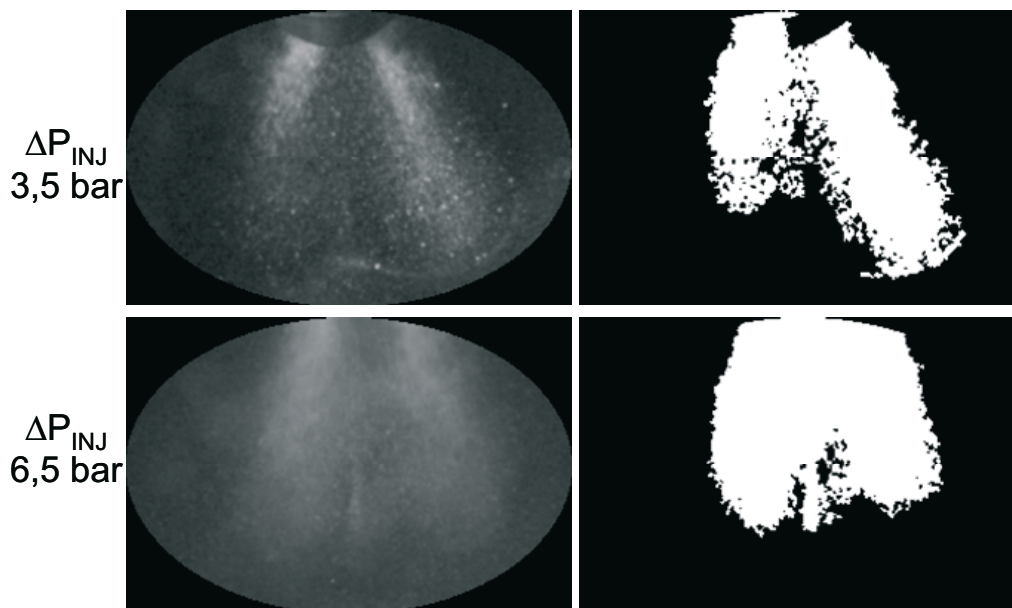


Fig. 6. Comparison between the binary digitizations of the fuel sprays detected for the selected injection pressures in closed valve condition at 8 ms from SOI

3.3. Combustion Process Analysis

The in-cylinder pressure measurements and the derived engine parameters are suitable for real-time measurement and control of the combustion process. On the other hand, they are not able to provide local and detailed information on thermal and fluid dynamic phenomena that occur in the combustion chamber. Thus, the optical techniques were applied. In particular UV-visible flame emission images were detected in the combustion chamber from the start of spark until the opening of the exhaust valves (around 155 CAD ATDC).

The flame propagation is governed by the local thermodynamic conditions and mixture composition as well as the local turbulence intensity[4]. However, the spatial evolution of the flame is a result of the superimposed effects of turbulent flame propagation, volumetric expansion of the hot combustion products behind the flame front and of the convective effects of the in-cylinder flow field. In addition, the in-cylinder flow field during combustion evolution is altered by the combustion process, but also by its interaction with the piston geometry. Squish regions and spark plug location exhibit a significant impact on the flame shape and its evolution characteristics [4].

It must be considered that the change in the injection pressure doesn't influence the turbulence level in the combustion chamber, but only the air-fuel mixing. Thus the proposed injection strategies have a general applicability and strong flexibility.

As previously observed in optical investigations performed in similar engine conditions, the flame propagation started from the spark location with nearly radial shape. The first evidence of the flame was detectable around 2 CAD after the spark timing (CAD ASOS) [5, 6]. The flame kernel evolved with a high cycle-to-cycle variation for about 10 CAD. Then a fully established self sustaining turbulent flame was observed until around 16 CAD ASOS. Analogous results are reported in Fig. 7 that shows the flame propagation for the different operating conditions. For the closed valves injection the region between the intake valves seemed to be off-limit for the flame[5,6]. This effect was due to fuel film deposited on the intake ports, caused by the fuel jet impingement on the intake manifold walls. Once formed, the fuel deposits developed dynamically under the influence of the gas flow. The heat exchange between the intake ports and the surrounding gas led to the fuel evaporation. The fuel deposit influenced the combustion process and the composition of the mixture creating locally rich-zones [7-10].

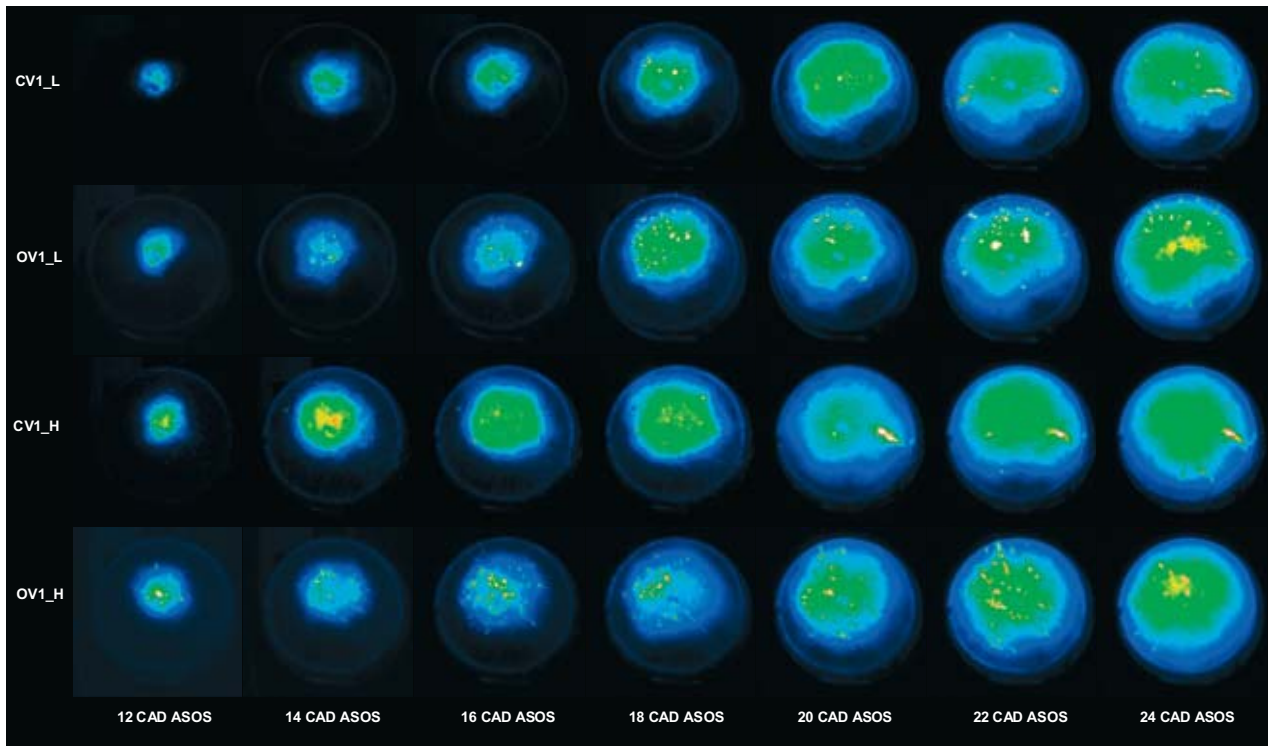


Fig. 7. Flame emission images detected in the combustion chamber

During the flame propagation, independently from the fuel deposit on the valves, the wall thermal boundary layer grew and the temperature of the unburned gas rose, due to the compression carried out by the expanding flame. The end gas in front of the flame was progressively more compressed and constrained by the solid boundary. Thus, the flame speed decreased from its highest value, dominated by the gas expansion in the middle of the volume burnt, to a value more dependent on the turbulent burning rate. As a consequence, the flame radius changed its trend and increased more slowly.

Fig. 8 reports the evolution of the flame radius for the selected engine conditions. Until 10 CAD ASOS, the fuel injection strategies had similar trends in the flame propagation. Higher flame speed was measured for the high pressure injection strategy. This result demonstrated that the good vaporization of small amounts of fuel could increase the flame speed from the kernel inception. This effect reduced the kernel cyclic variability and had strong influences on the further development of the combustion process increasing the flame stability[11-12].

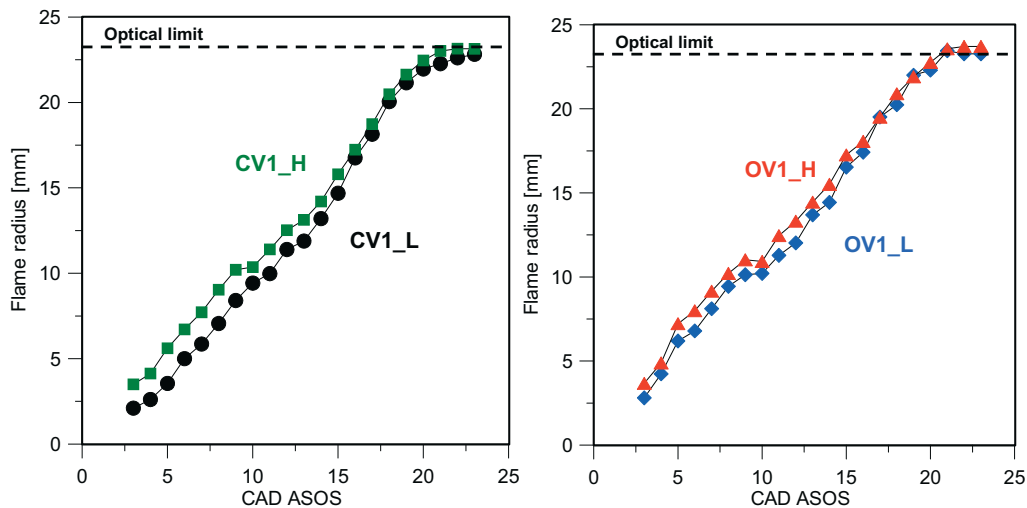


Fig. 8. Time evolution of the mean flame radius

The optical results obtained in the combustion chamber were compared with exhaust gas measurements. The unburned hydrocarbons (HC) and particulate matter (PM) concentration are reported in Table 4 for all the investigated engine operating conditions.

A reduction in PM and HC was detected for the open valves condition, this indicated a more complete combustion process due to the lower amount of the fuel deposited. The increase in injection pressure strongly reduced the particulate mass concentration. This is due to the better fuel mixing at high injection pressure, which allows a more efficient combustion process. In closed valves condition, the increase in HC at increasing injection pressure is due to the higher jet penetration that facilitates the formation of fuel deposits.

Tab. 4. HC and Particulate Mass emissions measured at the exhaust

Test	HC [g/kWh]	PM [mg/m ³]
CV1L	8.1	50.2
CV1H	9.0	33.8
OV1L	7.5	17.0
OV1H	6.7	6.8

4. Conclusions

In this work, it was investigated the effect of the fuel injection strategies on the combustion process and on the pollutant formation in a spark ignition boosted engine. Different injection strategies were considered. In particular, it was proposed the fuel injection with „open intake valves” rather than „closed”; 3.5 and 6.5 bar fuel injection pressures were tested. The experiments were performed on a partially transparent single-cylinder PFI SI engine, equipped with an optically accessible intake manifold and external boost device. The engine worked at WOT, MBT and stoichiometric equivalent ratio.

The combined study of global measurements and of the high spatial and temporal resolution optical results, showed an improvement in specific fuel consumption and emissions for the open valves condition without penalty in the engine performance. All these advantages were further improved by the increase in the injection pressure. These results were due to the better air-fuel mixing in the intake manifold that contributed to optimise the combustion process as shown by the optical results. The change in the injection phasing and pressure does not influence the turbulence level in the combustion chamber. Thus, the proposed injection strategies are low cost solutions with general applicability and strong flexibility.

Acknowledgments

The authors thank Mr. Carlo Rossi and Mr. Bruno Sgammato for their precious help and technical support.

References

- [1] Heywood, J. B., *Internal Combustion Engine Fundamentals.*, New York: McGraw-Hill 1988.
- [2] Zhu, G. G., Daniels, C. H., Winkelman J. - *MBT timing detection and its closed-loop control using in-cylinder pressure signal* – SAE, paper n. 2003-01-3266, 2003.
- [3] Heywood, J. B., Kasseris, E., *Comparative Analysis of Automotive Powertrain Choices for the Next 25 Years*, SAE paper n. 2007-01-1605, 2007.

- [4] Tatschl, R., Bogensperger, M., Kotnik, G., Priesching, P., Gouda, M., *Flame Propagation and Knock Onset Analysis for Full Load SI Engine Combustion Optimisation using AVL FIRE*, IMEM Users Group, SAE Congress, MI 2005.
- [5] Merola, S. S., Vaglieco, B. M., Formisano, G., Lucignano, G., Mastrangelo, G., *Flame Diagnostics in the Combustion Chamber of Boosted PFI SI Engine*, SAE Paper No. 2007-24-0003, 2007.
- [6] Merola, S. S., Sementa, P., Tornatore, C., Vaglieco, B.M., *Effect of fuel film deposition on Combustion Process in PFI SI engine*, Journal of Kones, Powertrain and Transport, Vol. 14, No. 3, 395-402, 2007.
- [7] Costanzo, V. S., Heywood, J. B., *Mixture Preparation Mechanisms in a Port Fuel Injected Engine*, SAE paper n. 2005-01-2080, 2005.
- [8] Gold, M. R., Arcoumanis, C., Whitelaw, J. H., Gaade, J.; Wallace, S., *Mixture Preparation Strategies in an Optical Four-Valve Port-Injected Gasoline Engine*, Int. J. of Engine Research, Vol. 1, No. 1, 41-56, 2000.
- [9] Shin, Y., Cheng, W. K., Heywood, J. B., *Liquid Gasoline Behaviour in the Engine Cylinder of a SI Engine*, SAE Paper n. 941872, 1994.
- [10] Zhu, G. S., Reitz, R. D., Xin, J., Takabayashi, T., *Modelling Characteristics of Gasoline Wall Films in the Intake Port of Port Fuel Injection Engines*, Int. J. of Engine Research, Vol. 2, No. 4, 231-248, 2001.
- [11] Bianco, Y., Cheng, W., Heywood, J. B., *The Effects of Initial Flame Kernel conditions on Flame Development in SI Engines*, SAE paper n. 912402, 1991.
- [12] Witze, P., Hall, M., Bennet, M., *Cycle-resolved Measurements of Flame Kernel Growth and Motion Correlated with Combustion Duration*, SAE paper n. 900023, 1990.

